Proc. Natl. Acad. Sci. USA
Vol. 93, pp. 14146–14151, November 1996
Neurobiology

Coexpression of *Drosophila* TRP and TRP-like proteins in *Xenopus* oocytes reconstitutes capacitative Ca^{2+} entry

(signal transduction/phosphoinositide signaling/*trp* mutant/calcium stores)

B. GILLO*†, I. CHORNA*†, H. COHEN*†, B. COOK*†, I. MANISTERSKY†‡, M. CHOREV§, A. ARNON*†, J. A. POLLOCK¶, Z. SELINGER*‡, AND B. MINKE*†‖

Departments of *Physiology, §Pharmaceutical Chemistry, ‡Biological Chemistry and the †Kühne Minerva Center for Studies of Visual Transduction, The Hebrew University, Jerusalem 91120, Israel; and ¶Department of Biological Sciences, Carnegie Mellon University, Pittsburgh, PA 15213-3890

Communicated by Denis Baylor, Stanford University School of Medicine, Stanford, CA, September 12, 1996 (received for review July 26, 1996)

ABSTRACT **Capacitative Ca^{2+} entry is a component of the inositol-lipid signaling in which depletion of inositol 1,4,5-trisphosphate ($InsP_3$)-sensitive Ca^{2+} stores activates Ca^{2+} influx by a mechanism that is still unknown. This pathway plays a central role in cellular signaling, which is mediated by many hormones, neurotransmitters, and growth factors. Studies of *Drosophila* photoreceptors provided the first putative capacitative Ca^{2+} entry mutant designated transient receptor potential (*trp*) and a *Drosophila* gene encoding TRP-like protein (*trpl*). It is not clear how the Ca^{2+} store depletion signal is relayed to the plasma membrane and whether both TRP and TRPL participate in this process. We report here that coexpressing *Drosophila* TRP and TRPL in *Xenopus* oocytes synergistically enhances the endogenous Ca^{2+}-activated Cl^- current and produces a divalent inward current. Both of these currents are activated by Ca^{2+} store depletion. In the absence of Ca^{2+}, Mg^{2+} is the main charge carrier of the divalent current. This current is characterized by lanthanum sensitivity and a voltage-dependent blocking effect of Mg^{2+}, which is relieved at both hyperpolarizing (inward rectification) and depolarizing (outward rectification) potentials. The store-operated divalent current is neither observed in native oocytes nor in oocytes expressing either TRP or TRPL alone. The production of this current implicates a cooperative action of TRP and TRPL in the depletion-activated current.**

Stimulation of many cell types by hormones, neurotransmitters, and growth-factors activates the inositol-lipid pathway leading to release of Ca^{2+} from intracellular stores. This Ca^{2+} release is followed by an influx of extracellular Ca^{2+} via a capacitative Ca^{2+} entry (CCE) mechanism (1). It has been suggested that activation of the surface membrane Ca^{2+} channels is caused by the depletion of Ca^{2+} in the internal stores and not by the release per se (1–8). Although CCE has been described in a large variety of cells and tissues (summarized in refs. 5 and 9), its mechanism of activation and molecular components is largely unknown. Visual transduction in *Drosophila*, which is triggered by the inositol lipid signaling (reviewed in refs. 10–13) has been suggested by Minke and Selinger (14) as a powerful model system to study CCE. This suggestion was based on the properties of a *Drosophila* mutant designated transient receptor potential *trp* (15, 16). In the *trp* mutant the photoreceptor potential declines to baseline during prolonged intense illumination and renders the photoreceptor cell inactive. The receptor potential recovers within 1 min in the dark (17). Because lanthanum (La^{3+}), a known non-specific blocker of Ca^{2+} channels, mimics many aspects of the *trp* phenotype in wild-type flies (18, 19), it has been suggested that *trp* has defects in Ca^{2+} entry into the photoreceptor cells (14). This prediction has been strongly supported by subsequent experiments demonstrating that the high Ca^{2+} permeability of the light-activated channels (20, 21) is reduced by about 10-fold in the *trp* mutant (22). Furthermore, fluorimetric measurements of cellular Ca^{2+} (23, 24) and measurements of a reduction in extracellular Ca^{2+} (25) have shown that Ca^{2+} influx is reduced by about 3-fold in the *trp* mutant relative to wild-type *Drosophila*, suggesting that TRP takes part in the main route of Ca^{2+} entry into the photoreceptor cells (10, 13, 14).

Molecular cloning of *Drosophila trp* (26, 27) and a related *Drosophila* gene designated transient receptor potential-like, *trpl* (28), revealed that their putative transmembrane domain exhibits weak but significant similarity to the α-subunit of the voltage-gated Ca^{2+} channel (28). Recently, a *trpl* mutant lacking TRPL has been isolated by Zuker and colleagues (29). The *trpl* mutant has a receptor potential similar to wild type and it reveals a strong phenotype only in a *trp* background. Thus, the double mutant *trpl;trp* is almost totally unresponsive to light (29). This study has suggested that TRP and TRPL are capable of responding to light activation independently of each other, but it does not exclude the possibility that TRP and TRPL form a multimeric channel (29). Additional subunit might exist but its function should depend on the presence of TRP and TRPL. Molecular and physiological data on TRP led a number of investigators to express the *Drosophila* TRP or TRPL in insect Sf9 cells (30, 31) or human homologue genes of *trp* (32, 33) in COS, Chinese hamster ovary, and Sf9 cells (9, 34). The heterologously expressed TRPL forms a constitutively active non-selective cation conductance, which could be enhanced by activation of the inositol lipid cascade (31, 35, 36). Heterologous expression of *Drosophila* TRP forms a conductance, which is activated by Ca^{2+} store depletion following treatment with the microsomal Ca^{2+} ATPase inhibitor, thapsigargin (30, 37, 38). Expression of *Drosophila* TRP in *Xenopus* oocytes enhances the endogenous Ca^{2+}-activated Cl^- conductance following depletion of the inositol 1,4,5-trisphosphate ($InsP_3$)-sensitive Ca stores (37). Recently, six *trp*-related genes of the mouse genome were identified in addition to new human homologues of *trp*. The expressed human gene products enhanced Ca^{2+} influx following Ca^{2+} store depletion (9, 34). Furthermore, expression in L cells of small portions of the mouse *trp* genes, in antisense orientation, suppressed the endogenous capacitative Ca^{2+} entry (9).

Here we report that heterologous coexpression of *Drosophila* TRP and TRPL in *Xenopus* oocytes synergistically enhanced the endogenous Ca^{2+}-activated Cl^- current upon Ca^{2+} stores depletion. In addition, the coexpressed TRP and TRPL

The publication costs of this article were defrayed in part by page charge payment. This article must therefore be hereby marked "*advertisement*" in accordance with 18 U.S.C. §1734 solely to indicate this fact.

Abbreviations: CCE, capacitative Ca^{2+} entry; $InsP_3$, inositol 1,4,5-trisphosphate; $InsP_3$-F, inositol 1,4,5-trisphosphate, 3-deoxy-3-fluoro; TRP, transient receptor potential protein; TRPL, TRP-like protein; LIC, light-induced current.

‖To whom reprint requests should be addressed.

produced a novel divalent cation current, which was activated by store depletion but could not be similarly activated when either TRP or TRPL were individually expressed. These findings strongly suggest a cooperative action of TRP and TRPL in the depletion-activated current.

MATERIALS AND METHODS

Analysis of Heterologous Expression of TRP and TRPL. The *trp* (26, 27) and *trpl* (28) cDNAs were subcloned into PGEMHE expression vector, which was constructed for expression in *Xenopus* oocytes (39, 40). Capped cRNA was synthesized *in vitro* and tested by translation in a rabbit reticulocyte lysate system before injection into oocytes. An amount of 0.2 mg/ml *trp*, 0.02 mg/ml *trpl*, and 0.2 mg/ml *trp* in combination with 0.02 mg/ml *trpl* cRNA, all in final volume of 50 nl, were injected into oocytes. The efficiency of translation of the *trp* and *trpl* cRNAs in oocytes was tested by Western blots on days 3–5 after injection. Aliquots equivalent to three oocytes were used for Western blot analyses. Aliquots equivalent to three *Drosophila* heads were used as markers for TRP and TRPL proteins (Fig. 1). Monoclonal anti-TRP antibody (mAb83F6) (41) and affinity-purified rabbit polyclonal anti-TRPL antibodies raised against the C-terminal hexadeca peptide of TRPL and enhanced chemiluminescense (Amersham) were used to visualized the TRP and TRPL proteins (Fig. 1).

Fluorescent Measurements of Ca^{2+} Changes. Fluorescent confocal Ca^{2+} measurements and electrophysiological studies were carried out 3–5 days after injection of cRNAs into oocytes. Oocytes were maintained and examined as described (42). Non-injected (control) oocytes or oocytes injected with cRNA encoding TRP, TRPL, and their combination (TRP+TRPL) were loaded with 50 μM of fluo-3 and 50 μM Fura Red (Molecular Probes). Control oocytes injected with 50 nl of cRNA buffer gave results indistinguishable from those of non-injected oocytes. Fluorescent dyes were injected approximately 20 min before the measurements together with 10 μM inositol 1,4,5,-trisphosphate 3-deoxy-3-fluoro ($InsP_3$-F) (final concentration, Sigma). The oocytes were bathed in Ca^{2+}-free ND96 medium containing: 96 mM NaCl, 2 mM KCl, 5 mM Hepes, 10 mM $MgCl_2$, 0.2 mM EGTA. Intracellular Ca^{2+} changes were measured before and during Ca^{2+} application and after washout of the Ca^{2+}-containing solution. In the Ca^{2+}-containing solution, EGTA was replaced with 2 mM $CaCl_2$ and $MgCl_2$ was reduced to 1 mM. Data acquisition was performed using the Sarastro confocal laser scanning microscope where the excitation light was 488 nm, the dichroic mirror was LP595, and the emission filters were 640DF35 and 530DF30 (Omega Optical, Brattleboro, VT) for the Fura Red and fluo-3 fluorescence, respectively. Scans included 512 × 512 pixels, with a pixel size of 2 μm using the Pl Fl 10/0.30 (Leitz) objective lens and a pinhole of 100 mm. Ratios were calculated as F640/F530 fluorescence. All oocytes were also tested electrophysiologically after the fluorescence measurements and gave results similar to those presented in Fig. 3.

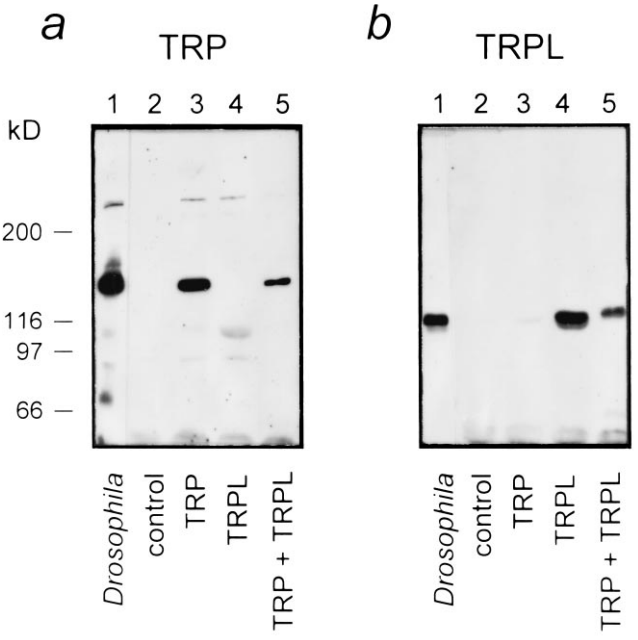

FIG. 1. Heterologous expression of TRP and TRPL gives rise to large amounts of TRP and TRPL proteins. Western blots show the expression of TRP (*a*) and TRPL (*b*) in oocytes injected with cRNA of *trp*, *trpl*, and *trp*+*trpl*, as indicated. Control (uninjected oocytes) and extract of three wild-type *Drosophila* heads (*Drosophila*) show that the equivalent molecular sizes of the *Drosophila* TRP and TRPL were produced in the oocytes, which cannot be confused with endogenous oocyte protein of similar structure and size. The data of this figure were highly reproducible in oocytes from different frogs (n = 8).

Electrophysiological Measurements Using Voltage-Clamped Oocytes. For electrophysiology, oocytes were impaled with two glass microelectrodes, which were filled with 3 M KCl with a resistance of 0.5–2.0 MΩ. The cells were voltage clamped using the standard two electrode-voltage-clamp technique. Drugs were added externally to the perfusate, while $InsP_3$-F (10 mM, final concentration) was injected into the oocyte with a Drummond 10 ml microdispenser. The small differences between the histograms of Fig. 3 *c* and *d* and the summary histogram of Fig. 5 arise from differences in the quality of the oocytes used in the various experiments. The most significant results were obtained in oocyte groups showing no deterioration with age and minimal leak currents.

Whole-Cell Recordings of Light-Induced Current (LIC) in *Drosophila*. Current-voltage relationship of the leak-subtracted peak LIC were plotted from responses to identical 100 ms light flashes of orange light (OG 590, Schott edge filter). The LICs were measured from *Drosophila* isolated ommatidia during whole-cell voltage clamp recordings as described (22, 23). Bath solution contained: 120 mM NaCl, 5 mM KCl, 10 mM TES buffer (pH 7.15), 30 mM sucrose, 8 $MgSO_4$, with no Ca^{2+} added. The whole-cell recording pipette contained: 100 mM CsCl, 15 mM TEA, 2 mM $MgSO_4$, 10 mM TES buffer (pH 7.15), 4 mM MgATP, 0.4 mM Na_2GTP.

RESULTS

Western Blot Analysis Showing Expression of TRP and TRPL. Expression of TRP and TRPL proteins in *Xenopus* oocytes microinjected with cRNA to their respective genes was demonstrated by Western blot analysis using monoclonal anti-TRP antibody (41) (Fig. 1*a*) or affinity-purified anti-TRPL antibody (Fig. 1*b*). We have found that high levels of TRPL expression largely reduced the survival time of the oocytes and, therefore, the level of TRPL expression should be carefully controlled. In contrast, the expression level of TRP had no effect on the survival time of the oocytes. Accordingly, we injected a 10-fold larger amount of cRNA encoding TRP than TRPL. The significant reduction in expression of TRP or TRPL in oocytes coexpressing TRP+TRPL is probably due to competition on the protein synthesis system of the oocyte.

Fluorescent Measurements of Ca^{2+} Changes Reveal Enhanced Ca^{2+} Permeability in TRP+TRPL-Expressing Oocytes. Fluorescent Ca^{2+} indicators were used to detect intracellular Ca^{2+} changes in oocytes expressing TRP, TRPL, or both (TRP+TRPL, Fig. 2). CCE was induced by depletion of the $InsP_3$-sensitive Ca^{2+} stores and measured as a change in intracellular Ca^{2+} following application of Ca^{2+} to the external medium. Confocal images of Fura Red/fluo-3 ratio difference revealed an enhanced rise in cytoplasmic Ca^{2+} in

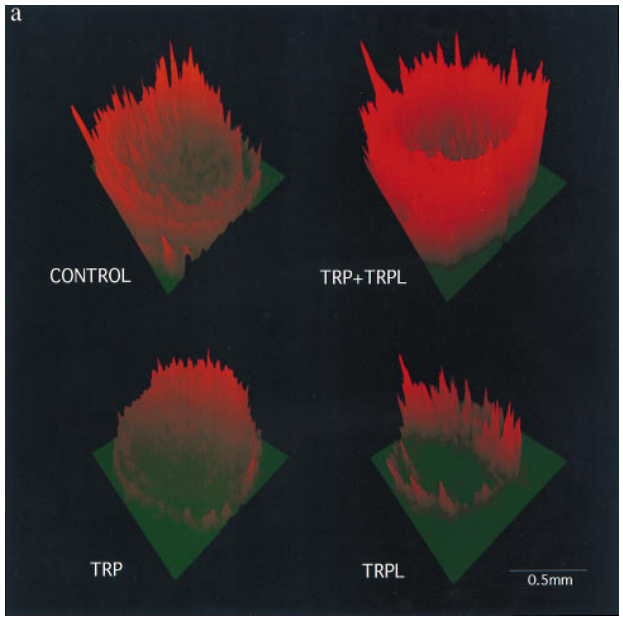

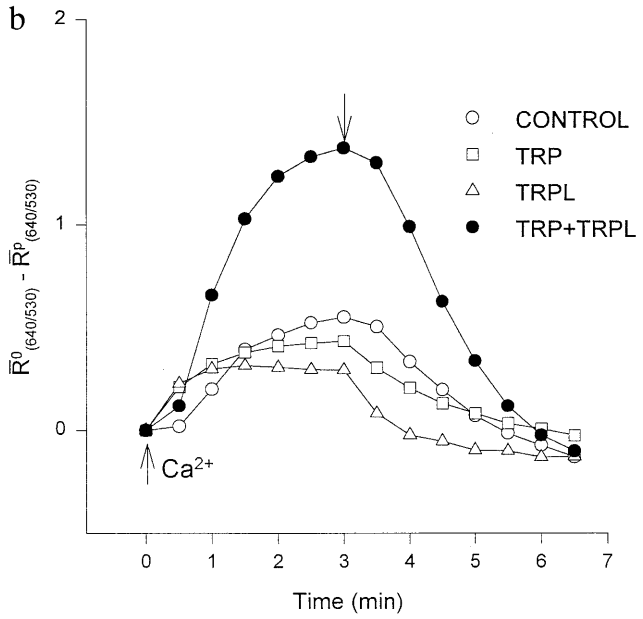

FIG. 2. Coexpression of TRP and TRPL largely enhances Ca^{2+} influx into Ca^{2+} stores-depleted oocytes. (*a*) Confocal images of ratio changes between resting and peak Ca^{2+} levels during application of Ca^{2+} containing solution (2 mM). Changes of ratios were coded as the green-to-red gradient together with the *z*-axis magnitude. One pair of optical sections across the oocyte of about 70 μm deep was analyzed to form each image. The "ring" shape of the image is due to the melanin pigmentation, which interferes with the fluorescence detection from the center of the oocyte. (*b*) A plot of changes in fluorescence ratio as a function of time in the oocytes shown in *a*. The ordinate plots the average ratio difference ($\bar{R}^{o}_{(640/530)} - \bar{R}^{P}_{(640/530)}$) where $\bar{R}$ is the averaged fluorescence ratio of the scan before ($\bar{R}^{o}$) or during and after ($\bar{R}^{P}$) Ca^{2+} application. The ratio of the pixels was averaged for a whole scan after threshold noise reduction. The normalized average ratio difference of TRP+TRPL was 2.08 ± 0.23 ($n = 5$) times the averaged control ($n = 9$), as compared with TRPL alone at 0.82 ± 0.10 ($n = 5$) times the control. The TRP+TRPL group was significantly different from the other oocyte groups ($P < 0.01$), whereas the other oocyte groups were not significantly different ($P > 0.05$). The initial Ca^{2+} level was variable among oocytes; therefore, ratio differences were used to demonstrate consistent results similar to those shown in Fig. 3 *b* and *c*. The magnitude of the ratio differences varied in different experiments; therefore, the summary results were normalized. The time of Ca^{2+} application and removal is indicated by up- and down-pointing arrows, respectively.

TRP+TRPL-expressing oocytes (Fig. 2*a*). Spatial averages of fluorescence ratios at different times are shown in Fig. 2*b*. The oocytes expressing TRP+TRPL showed a 2- to 3-fold larger increase in cytoplasmic Ca^{2+} than did control oocytes or oocytes individually expressing either TRP or TRPL, suggesting a larger Ca^{2+} permeability of the TRP+TRPL-expressing oocytes (Fig. 2*b*). The Western blots (Fig. 1) indicate that the large response of the TRP+TRPL system (Fig. 2) could not be due to excessive expression of either TRP or TRPL.

Functional Coexpression of TRP+TRPL Produced Capacitative Ca^{2+} Entry Currents. To analyze CCE oocytes were bathed in Ca^{2+}-free medium and the $InsP_3$-sensitive Ca^{2+} stores were depleted of Ca^{2+} either by treatment with thapsigargin (1 μM) for ≈2 hr before the measurements, or by intracellular injection of $InsP_3$-F (10 μM). This procedure totally eliminated intracellular calcium as verified by subsequent injection of $InsP_3$-F (10 μM), which failed to induce any response ($n = 8$) (43, 44). An increase in cellular Ca^{2+} produces a large native Ca^{2+}-activated Cl^- current ($I_{Cl,Ca}$), which interferes with direct Ca^{2+} current measurements (37, 44–46). Therefore, two independent procedures were used to assess divalent cation permeability: (*i*) endogenous $I_{Cl,Ca}$ was used as a sensitive reporter for an increase in cellular Ca^{2+} (Fig. 3*a*), (*ii*) a novel inward current carried mainly by Mg^{2+}, (referred to as *Drosophila* store-operated current, I_{dSOC}) was measured in the absence of external and internal Ca^{2+}. A prior injection of 2 mM EGTA (final concentration, $n = 7$, see Fig. 3*b*) ensured that the internal Ca^{2+} stores were totally depleted.

$I_{Cl,Ca}$ was activated by a Ca^{2+} pulse, followed by a voltage step from holding voltage of −10 mV to −120 mV in Ca^{2+} store-depleted oocytes. The voltage step increased the driving force for Ca^{2+} influx. An instantaneous leak current followed by a transient inward $I_{Cl,Ca}$ current with well-described characteristics was measured (44, 45). A relatively small $I_{Cl,Ca}$ was observed in non-injected (control) oocytes or in oocytes expressing TRP (Fig. 3*a*, but see Fig. 5*a*). Oocytes expressing TRPL revealed a dependence of $I_{Cl,Ca}$ on the chemical agent used for Ca^{2+} store depletion (see below, Figs. 3 *a* and *c* and 5*a*). Oocytes expressing TRP+TRPL showed the largest $I_{Cl,Ca}$ (Figs. 3 *a* and *c* and 5*a*).

Properties of the Depletion-Activated Divalent Current. To measure I_{dSOC} in Ca^{2+} store-depleted oocytes the holding voltage (−10 mV) was stepped to −120 mV in the presence of 10 mM external Mg^{2+} and Ca^{2+}-free medium. The store-depletion-activated I_{dSOC} was observed only in oocytes expressing TRP+TRPL (Figs. 3 *b* and *d* and 5*b*). Lanthanum, an efficient blocker of the *trp*-dependent conductance in *Drosophila* photoreceptors (19, 22) completely and reversibly blocked $I_{Cl,Ca}$ and I_{dSOC} (Fig. 3 *c* and *d*). I_{dSOC} had a slow rise time of ≈3 min ($n = 6$); also, it did not decline during the negative voltage step. These properties of I_{dSOC} may arise from a partial voltage-dependent blocking effect of Mg^{2+} (see below) that was slowly removed by the large hyperpolarizing voltage step and from the absence of Ca^{2+}-mediated negative feedback, respectively. Ca^{2+}-mediated negative feedback is typical for $InsP_3$ systems (5, 43).

The current-voltage relationship (I-V curve) of $I_{d_{SOC}}$ (Fig. 4) showed an increased inward current below −80 mV (inward rectification) and outward current above 30 mV (outward rectification). Similarly, the *Drosophila* LIC shows an I-V curve with inward and outward rectification (22, 41) (Fig. 4, *Inset*). When Na^+ was replaced with the impermeable cation *N*-methyl-D-glucamine at 10 mM external Mg^{2+} no significant effect on the I-V curve was observed. This suggests that Mg^{2+} is the main cationic charge carrier of I_{dSOC} (Fig. 4). However, Mg^{2+} had an inhibitory effect on the amplitude of I_{dSOC} showing a decrease in inward current when external Mg^{2+} was increased. Thus, the dependence of I_{dSOC} on external Mg^{2+} concentration is complex and requires further study. There are quantitative differences between the *Drosophila* LIC and

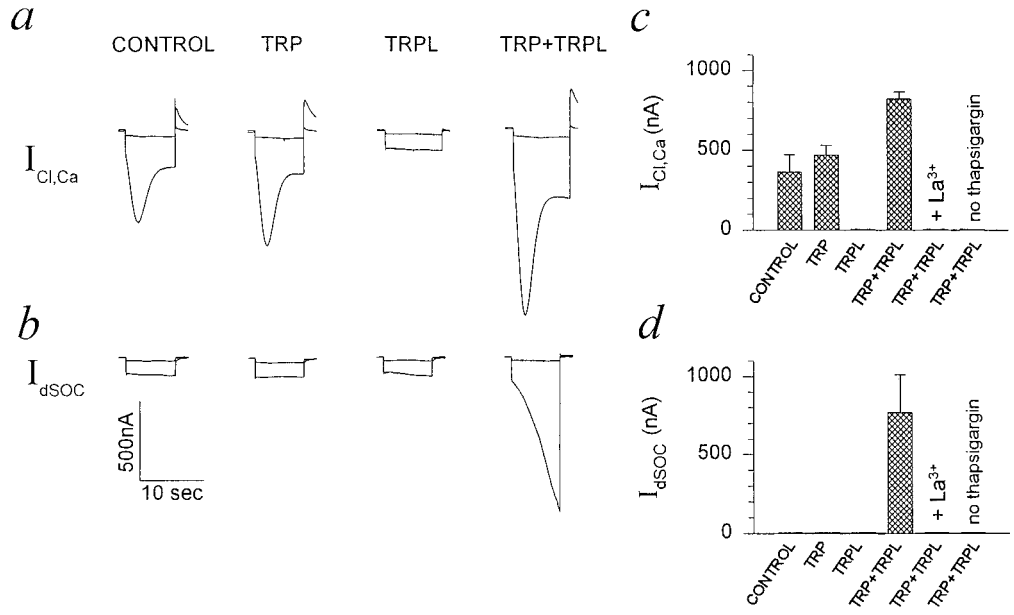

FIG. 3. Functional coexpression of TRP+TRPL in *Xenopus* oocytes produced a capacitative Ca^{2+} entry system revealed by $I_{Cl,Ca}$ and I_{dSOC}. Shown is a single experiment, employing several oocytes from a single frog that were maintained and treated together. (*a*) Measurements of currents ($I_{Cl,Ca}$) in thapsigargin-treated oocytes (1 μM in Ca^{2+}-free solution for 1.5–2 hr). $I_{Cl,Ca}$ was activated by stepping the holding voltage from −10 mV to −30 mV (upper traces) and to −120 mV (bottom traces) to show the relatively small instantaneous leak current in solution containing 1 mM Ca^{2+} (see Fig. 2). Oocytes were injected with cRNA 5 days before the measurements. (*b*) Measurements of I_{dSOC} were carried out as described in *a*. The same oocytes were perfused with Ca^{2+}-free ND96 solution (10 mM Mg^{2+}). In some of the measurements, 2 mM EGTA was injected into the oocytes 1–2 hr before the recordings, but no significant effect on I_{dSOC} was found. I_{dSOC} was totally and reversibly blocked by addition of 1 mM La^{3+} to the perfusate (*c* and *d*). I_{dSOC} was also blocked reversibly by 500 μM, but not by 50 μM, La^{3+} ($n = 12$). (*c* and *d*) Histograms summarizing the results from all the oocytes of the same experimental run of *a* and *b*. Five to 10 oocytes were used for each of the experimental groups of *a* and *b*. The histograms present the mean and SEM of the peak $I_{Cl,Ca}$ (*c*) and maximal I_{dSOC} (*d*) measured at −120-mV holding potentials after the instantaneous leak currents were subtracted from all current traces. The TRP+TRPL group was significantly different from the other oocyte groups of *c* ($P < 0.01$). The control and TRP groups were not significantly different ($P > 0.05$).

I_{dSOC}. The LIC of *Drosophila* is more sensitive to La^{3+} (ref. 22, and see legend of Fig. 3*b*) and has a larger Na^+ permeability than $I_{d_{SOC}}$ of the oocytes expressing TRP+TRPL (22) (Fig. 4).

Without Ca^{2+} store depletion at non-toxic TRPL expression level (see below), neither $I_{Cl,Ca}$ (44) nor I_{dSOC} could be observed (Fig. 3 *c* and *d*) even with elevated external concentration of Ca^{2+} (10 mM, $n = 9$) or Mg^{2+} (40 mM, $n = 8$). Oocytes injected with a 10-fold larger dose of *trpl* cRNA showed a significant $I_{Cl,Ca}$ or inward Mg^{2+} current similar to I_{dSOC}; however, this current was activated by a negative voltage step without depletion of the Ca^{2+} stores ($n = 21$). The latter effect is reminiscent of a property of the currents that have been described in TRPL-expressing Sf9 cells, which show constitutively active cationic channels (30, 31, 36), but poor ability to conduct Mg^{2+}. However, these conditions were toxic and most of the oocytes died within 4 days depending on the expression level of TRPL.

The summary histogram in Fig. 5*a* shows that oocytes expressing TRP or TRPL exhibited a dependence of $I_{Cl,Ca}$ on the method of Ca^{2+} store depletion. In the TRPL-expressing oocytes, depletion using thapsigargin significantly reduced $I_{Cl,Ca}$ below the control level, whereas depletion using $InsP_3$-F enhanced the $I_{Cl,Ca}$ current above the level of the controls (Fig. 5*a*). In oocytes expressing TRP alone, thapsigargin treatment exhibited a significant increase in $I_{Cl,Ca}$ over control oocytes (37), which was not observed in $InsP_3$-F treated oocytes (Fig. 5*a*). The above differential effects are reminiscent of the results reported for Sf9 cells expressing individually TRP or TRPL (30, 31, 36). At present we do not have sufficient data to explain the effects of either TRP or TRPL on $I_{Cl,Ca}$ or the currents recorded in Sf9 cells. A possible explanation is that the effects shown in Fig. 5*a* are apparently due to individual interactions of TRP or TRPL with the endogenous CCE (8, 9). Such individual interactions may also account for the enhancement of the depletion-activated current described for Sf9 cells or $I_{Cl,Ca}$ recorded in oocytes expressing TRP alone (30, 37, 38). Oocytes expressing TRP+TRPL revealed approximately 3-fold larger $I_{Cl,Ca}$ than the controls regardless of the method used to deplete the Ca^{2+} stores (Fig. 5*a*). The summary histogram in Fig. 5*b* shows that under our experimental conditions the store-depletion activated I_{dSOC} was observed only in oocytes expressing TRP+TRPL.

DISCUSSION

The induction of the I_{dSOC} response to Ca^{2+} store depletion, in oocytes coexpressing *Drosophila* TRP+TRPL, clearly showed that these proteins are efficiently coupled to the endogenous store-depletion signal. Depletion of internal stores in *Drosophila* photoreceptors by thapsigargin fails to induce inward current in the dark (47). However, application of ionomycin together with Ca^{2+} chelators, a procedure that might be expected to deplete intracellular stores, leads to production of inward current in *Drosophila* photoreceptors suggesting that CCE does exist in *Drosophila* photoreceptors (R. C. Hardie, personal communication).

The most significant result of coexpressing TRP+TRPL was revealed by measuring I_{dSOC} and its voltage-dependent Mg^{2+} current showing inward and outward rectification (Fig. 4) in thapsigargin-treated oocytes. Similarly, the LIC of *Drosophila* has a permeability to Mg^{2+} (22), as well as a voltage-dependent blocking effect of Mg^{2+} (48). The creation of La^{3+}-sensitive Mg^{2+} current with inward rectification in the oocyte is thus similar to a unique characteristic of the *Drosophila* photoreceptor cell.

Unlike I_{dSOC}, capacitative Ca^{2+} entry current in various vertebrate cells is carried almost exclusively by Ca^{2+} (3, 4, 49–51; but also see ref. 52). It therefore appears that the

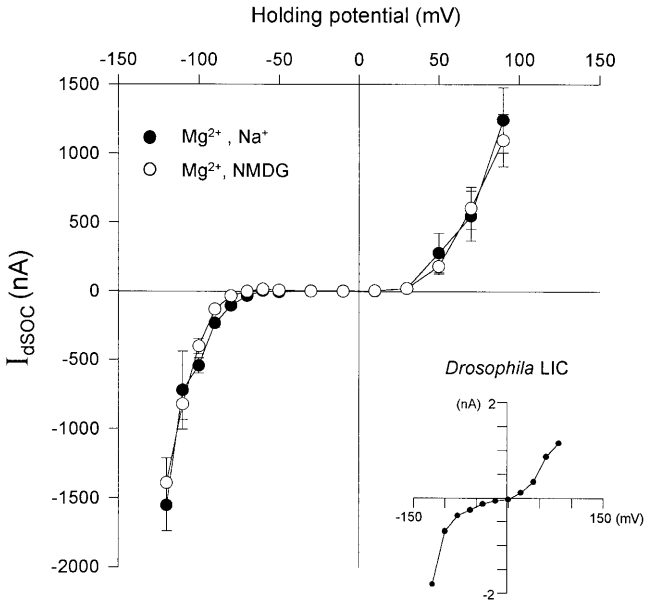

FIG. 4. Current-voltage relationship of I_{dSOC} in oocytes expressing TRP+TRPL. Inward and outward rectification typical of *Drosophila* light-activated current are shown. Current-voltage relationship (I-V curve) plotting the leak-subtracted maximal I_{dSOC} as a function of holding voltage in $InsP_3$-F (10 μM) or thapsigargin-treated oocytes incubated in Ca^{2+}-free medium (see Fig. 3 *a* and *b*). Solutions are as in Fig. 3*b*. The I-V curves were measured before (●) and after (○) Na^+ was replaced by *N*-methyl-D-glucamine (NMDG, 96 mM). Graphs show the average of currents obtained from nine oocytes of a single experiment. Very similar results were obtained in five other experiments. (*Inset*) Current-voltage relationship of the leak-subtracted peak LIC responses to identical 100-ms light flashes of orange light (OG 590, Schott edge filter) recorded from *Drosophila* isolated ommatidia during whole-cell voltage clamp recordings as described (22).

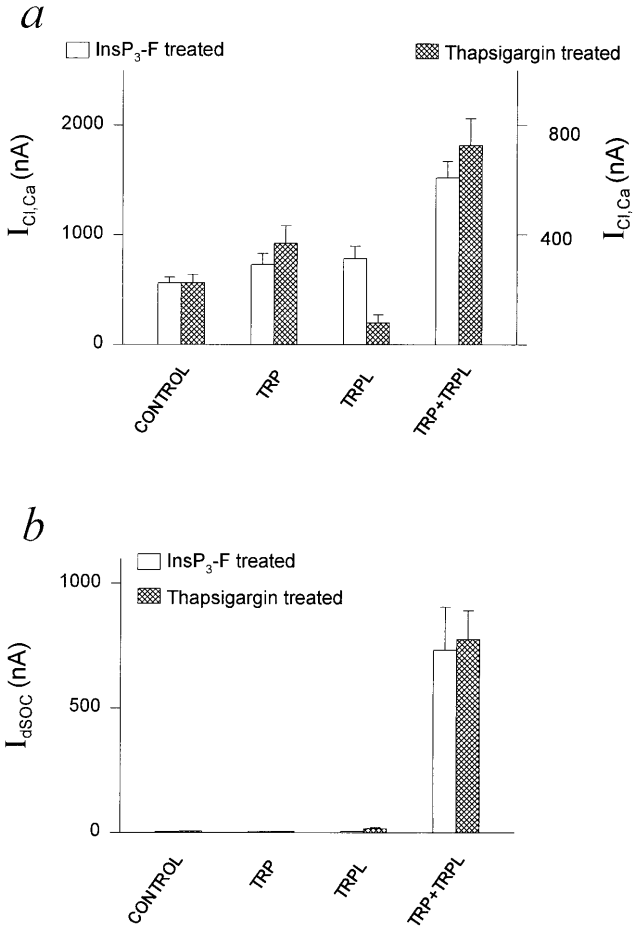

FIG. 5. Histograms summarizing $I_{Cl,Ca}$ and I_{dSOC} in TRP, TRPL, and TRP+TRPL-expressing oocytes in experiments similar to those in Fig. 3. (*a*) $I_{Cl,Ca}$ measured in $InsP_3$-F-treated oocytes (left ordinate) or thapsigargin-treated oocytes (right ordinate). Eleven independent experiments used 16–64 oocytes in each group. The TRP+TRPL groups were significantly different from the other oocyte groups ($P < 0.01$), whereas the other oocyte groups were not significantly different in the $InsP_3$-F-treated oocytes ($P > 0.05$). In the thapsigargin-treated oocytes all groups were significantly different from each other ($P < 0.01$ for a comparison between the control TRPL and TRP+TRPL groups; $P < 0.05$ for a comparison between the control and TRP group). (*b*) I_{dSOC} measured in $InsP_3$-F or thapsigargin-treated oocytes. Seven independent experiments used 8–22 oocytes in each group.

TRP+TRPL-dependent current has some properties different from the capacitative Ca^{2+} entry currents of several vertebrate cells (5, 7). I_{dSOC} is also different from the currents found in the Sf9 cells expressing either TRP or TRPL, which are characterized by a linear I-V curve, absence of a Mg^{2+} block of the TRP-dependent conductance; and a constitutive activity of the TRPL-dependent conductance. The coexpressed TRP+TRPL-dependent current in *Xenopus* oocyte suggests that we have reconstituted a capacitative Ca^{2+} entry mechanism with some similarity to the native *Drosophila* system. Our data suggest that a cooperative action of TRP and TRPL is efficiently coupled to the endogenous Ca^{2+} store-depletion signal. The synergistic activity of TRP and TRPL in the production of the depletion-activated current suggest that these proteins interact with each other (for a review see ref. 13). The simplest interpretation of our results is that TRP and TRPL contribute channel subunits to form a multimeric channel. Nevertheless, our results, as well as the individual expression of *Drosophila* TRP, TRPL, and the human *trp* homologue genes (9, 30, 31, 34–36) have not demonstrated that the various TRP proteins form ionic channels. It is still possible that these expressed proteins exert their function through the endogenous CCE channels (8, 9). Other approaches, such as coimmunoprecipitation of TRP and TRPL should be used in future experiments to demonstrate that the physiological synergism found in this study is based on physical interaction between the two proteins. Also, single-channel recordings should be made to study the identity and properties of the depletion-activated channels. This study has established a useful basis for such future studies.

We thank Dr. Roger C. Hardie for the permission to quote his unpublished results, Drs. Craig Montell and Len Kelly for the cDNA of *trp* and *trpl* in bluescript vector, and Arnd Baumann for the cDNA of the above genes in PGEMHE vector. We thank Drs. U. Benjamin Kaupp, Charles S. Zuker, and Roger C. Hardie for critical comments on an earlier version of the manuscript. We also thank O. Devary, L. Alfonte, M. Eshel, and G. Barkai for technical help. This research was supported by grants from the National Institutes of Health, the Kuhne Minerva Center, the U.S.–Israel Binational Science Foundation (B.M. and Z.S.), the German-Israel Foundation (B.M.), and grants from the National Institutes of Health and National Science Foundation–Center for Light Microscope Imaging and Biotechnology (J.A.P.)

1. Putney, J. W. J. (1990) *Cell Calcium* **11,** 611–624.
2. Hoth, M. & Penner, R. (1992) *Nature (London)* **355,** 353–356.
3. Zweifach, A. & Lewis, R. S. (1995) *J. Biol. Chem.* **270,** 14445–14451.
4. Lewis, R. S. & Cahalan, M. D. (1995) *Annu. Rev. Immunol.* **13,** 623–653.
5. Berridge, M. J. (1995) *Biochem. J.* **312,** 1–11.
6. Clapham, D. E. (1995) *Cell* **80,** 259–268.
7. Clapham, D. E. (1996) *Neuron* **16,** 1069–1072.
8. Friel, D. D. (1996) *Cell* **85,** 617–619.

9. Zhu, X., Jiang, M. S., Peyton, M., Boulay, G., Hurst, R., Stefani, E. & Birnbaumer, L. (1996) *Cell* **85,** 661–671.
10. Hardie, R. C. & Minke, B. (1995) *Cell Calcium* **18,** 256–274.
11. Ranganathan, R., Malicki, D. M. & Zuker, C. S. (1995) *Annu. Rev. Neurosci.* **18,** 283–317.
12. Pak, W. L. (1995) *Invest. Ophthalmol. Visual Sci.* **36,** 2340–2357.
13. Minke, B. & Selinger, Z. (1996) *Curr. Opin. Neurobiol.* **6,** 459–466.
14. Minke, B. & Selinger, Z. (1991) *Prog. Retinal Res.* **11,** 99–124.
15. Minke, B., Wu, C. & Pak, W. L. (1975) *Nature (London)* **258,** 84–87.
16. Cosens, D. J. & Manning, A. (1969) *Nature (London)* **224,** 285–287.
17. Minke, B. (1982) *J. Gen. Physiol.* **79,** 361–385.
18. Hochstrate, P. (1989) *J. Comp. Physiol. A.* **166,** 179–187.
19. Suss-Toby, E., Selinger, Z. & Minke, B. (1991) *J. Gen. Physiol.* **98,** 849–868.
20. Hardie, R. C. (1991) *Proc. R. Soc. London B* **245,** 203–210.
21. Ranganathan, R., Harris, G. L., Stevens, C. F. & Zuker, C. S. (1991) *Nature (London)* **354,** 230–232.
22. Hardie, R. C. & Minke, B. (1992) *Neuron* **8,** 643–651.
23. Peretz, A., Suss-Toby, E., Rom-Glas, A., Arnon, A., Payne, R. & Minke, B. (1994) *Neuron* **12,** 1257–1267.
24. Hardie, R. C. (1996) *J. Neurosci.* **16,** 2924–2933.
25. Peretz, A., Sandler, C., Kirschfeld, K., Hardie, R. C. & Minke, B. (1994) *J. Gen. Physiol.* **104,** 1057–1077.
26. Montell, C. & Rubin, G. M. (1989) *Neuron* **2,** 1313–1323.
27. Wong, F., Schaefer, E. L., Roop, B. C., LaMendola, J. N., Johnson Seaton, D. & Shao, D. (1989) *Neuron* **3,** 81–94.
28. Phillips, A. M., Bull, A. & Kelly, L. E. (1992) *Neuron* **8,** 631–642.
29. Niemeyer, B. A., Suzuki, E., Scott, K., Jalink, K. & Zuker, C. S. (1996) *Cell* **85,** 651–659.
30. Vaca, L., Sinkins, W. G., Hu, Y., Kunze, D. L. & Schilling, W. P. (1994) *Am. J. Physiol.* **267,** C1501–C1505.
31. Harteneck, C., Obukhov, A. G., Zobel, A., Kalkbrenner, F. & Schultz, G. (1995) *FEBS Lett.* **358,** 297–300.
32. Wes, P. D., Chevesich, J., Jeromin, A., Rosenberg, C., Stetten, G. & Montell, C. (1995) *Proc. Natl. Acad. Sci. USA* **92,** 9652–9656.
33. Zhu, X., Chu, P. B., Peyton, M. & Birnbaumer, L. (1995) *FEBS Lett.* **373,** 193–198.
34. Zitt, C., Zobel, A., Obukhov, A. G., Harteneck, C., Kalkbrenner, F., Lückhoff, A. & Schultz, G. (1996) *Neuron* **16,** 1189–1196.
35. Hu, Y., Vaca, L., Zhu, X., Birnbaumer, L., Kunze, D. L. & Schilling, W. P. (1994) *Biochem. Biophys. Res. Commun.* **201,** 1050–1056.
36. Dong, Y., Kunze, D. L., Vaca, L. & Schilling, W. P. (1995) *Am. J. Physiol.* **269,** C1332–C1339.
37. Petersen, C. C. H., Berridge, M. J., Borgese, M. F. & Bennett, D. L. (1995) *Biochem. J.* **311,** 41–44.
38. Sinkins, W. G., Vaca, L., Hu, Y., Kunze, D. L. & Schilling, W. P. (1996) *J. Biol. Chem.* **271,** 2955–2960.
39. Liman, E. R., Tytgat, J. & Hess, P. (1992) *Neuron* **9,** 861–871.
40. Baumann, A., Frings, S., Godde, M., Seifert, R. & Kaupp, U. B. (1994) *EMBO J.* **13,** 5040–5050.
41. Pollock, J. A., Assaf, A., Peretz, A., Nichols, C. D., Mojet, M. H., Hardie, R. C. & Minke, B. (1995) *J. Neurosci.* **15,** 3747–3760.
42. Gillo, B., Lass, Y., Nadler, E. & Oron, Y. (1987) *J. Physiol. (London)* **392,** 349–361.
43. Singer, D., Boton, R., Moran, O. & Dascal, N. (1990) *Pflügers Arch.* **416,** 7–16.
44. Petersen, C. C. & Berridge, M. J. (1994) *J. Biol. Chem.* **269,** 32246–32253.
45. Yao, Y. & Parker, I. (1993) *J. Physiol. (London)* **468,** 275–295.
46. Parekh, A. B., Terlau, H. & Stuhmer, W. (1993) *Nature (London)* **364,** 814–818.
47. Ranganathan, R., Bacskai, B. J., Tsien, R. Y. & Zuker, C. S. (1994) *Neuron* **13,** 837–848.
48. Hardie, R. C. & Mojet, M. H. (1995) *J. Neurophysiol.* **74,** 2590–2599.
49. Lewis, R. S. & Cahalan, M. D. (1989) *Cell Regul.* **1,** 99–112.
50. Zweifach, A. & Lewis, R. S. (1993) *Proc. Natl. Acad. Sci. USA* **90,** 6295–6299.
51. Penner, R., Fasolato, C. & Hoth, M. (1993) *Curr. Opin. Neurobiol.* **3,** 368–374.
52. Lückhoff, A. & Clapham, D. E. (1994) *Biophys. J.* **67,** 177–182.